



ORIGINAL ARTICLE

CS@Cu₂O and magnetic Fe₃O₄@SiO₂-pAMBA-CS-Cu₂O as heterogeneous catalysts for CuAAC click reaction



Fatemeh Jafarzadeh, Zahra Dolatkhah, Shiva Molaei, Shahrzad Javanshir*

Pharmaceutical and Heterocyclic Chemistry Research Laboratory, Department of Chemistry, Iran University of Science and Technology, Tehran 16846-13114, Iran

Received 2 January 2022; accepted 10 March 2022

Available online 14 March 2022

KEYWORDS

Click chemistry;
Bio-waste;
Corn Silk;
Heterogeneous catalysts;
Magnetic nanoparticles;
Triazole

Abstract The recovery of agricultural and food wastes are one of the main areas of current research for optimal biowaste management to reduce greenhouse gas (GHG) emissions that are generated when it is not properly treated. Corn silk (CS) as biowaste from the agricultural sector is a rich source of natural compounds especially polysaccharides. We present here a chemical activation method to convert CS to values added heterogeneous catalyst for the synthesis of triazoles compounds *via* copper catalyzed azide-alkyne cycloaddition (CuAAC) reaction. For this purpose, cuprous oxide coated CS (CS@Cu₂O) and multifunctional Fe₃O₄@SiO₂-*para*-aminomethyl benzoic acid-CS-Cu₂O composite (denoted as Fe₃O₄@SiO₂-pAMBA-CS-Cu₂O) were fabricated. Different analytical techniques have been used to describe the size, crystal structure, elemental composition and other physical properties of the fabricated catalysts. These heterogeneous catalysts showed excellent catalytic activities for the synthesis of 1,4-disubstituted-1,2,3-triazoles *via* click reaction in H₂O at 70 °C under base and external-reductant-free conditions. The magnetic properties of the catalyst allowed easy separation after reaction by simply applying an external magnet. Other advantages of this work are the recyclability of the catalyst, the absence of reducing agent and base, besides utilisation of bio wastes for the production of heterogeneous catalyst.

© 2022 The Authors. Published by Elsevier B.V. on behalf of King Saud University. This is an open access article under the CC BY license (<http://creativecommons.org/licenses/by/4.0/>).

1. Introduction

Growth of human population contributes to increasing demands for agricultural products and related products of food industry (Ravindran et al., 2021), (Usmani et al., 2020). In general, Bio-wastes emanate from 3 specific sources which are agricultural, municipal and industrial wastes (Ravindran et al., 2021). Bio-wastes originates from agricultural sources, mostly consists of livestock manure and crop residues.

* Corresponding author.

E-mail address: shjavan@iust.ac.ir (S. Javanshir).

Peer review under responsibility of King Saud University.



Production and hosting by Elsevier

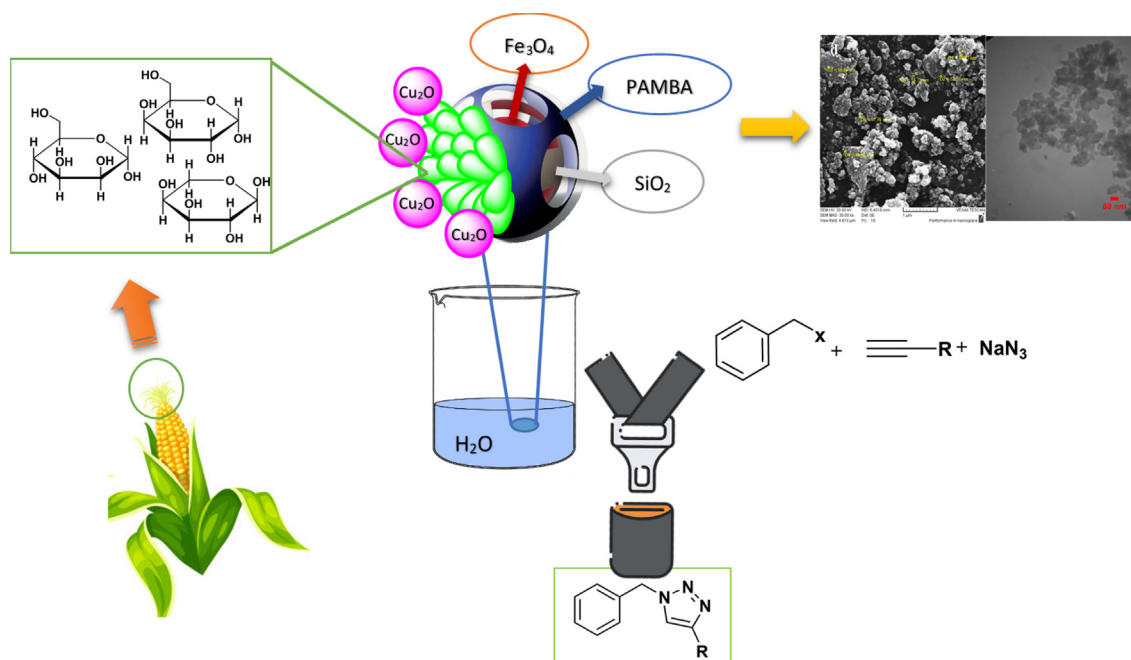
Agricultural and food industries generate enormous liquid and solid wastes which inability to effectively convert these materials into valuable substances can lead to environmental damage (Ravindran et al., 2021). This issue has led chemists to promote routes for reducing the amount of the pollutants and turn them into more valuable materials (Sun et al., 2021), (Athinarayanan et al., 2019). Scheme 1.

Corn is the one of the most versatile and widely consumed agricultural products around the world. CS, also known as *Maydis Stigma* or *Zea Mays*, is the waste of the corn. In fact, CS, the long shiny fibers at the top of an ear of corn, is one of the agricultural by-product (Rahman and Rosli, 2014). This Bio-waste is used as traditional medicine for treatment of diabetes and diuresis in China (Jia et al., 2021). It also has health benefits such as diuretic, antioxidant, anti-obesity, anti-coagulation, anti-tumor and it might alter blood sugar levels so used to treat diabetes, and help reduce inflammation (Hasanudin et al., 2012), (Liu et al., 2011), (Ren et al., 2013). This Bio-waste is a rich source of bioactive compounds such as proteins, carbohydrates, vitamins, minerals, fiber, and steroids such as sterols and stigma sterols, alkaloids, tannins and saponins (Jia et al., 2021; Hasanudin et al., 2012; Liu et al., 2011; Ren et al., 2013). In studies of the CS components has been shown that carbohydrates (67.3%) constitute of the bulk of its structure (Jia et al., 2021; Haslina et al., 2017). For this reason, this natural compound can be widely used as a carbohydrate structure that chemical modification of this bio-composite can be another effective way for the advancement of chemical biology and drug development (Choi et al., 2020). On the other hand, due to the presence of natural reducing compounds such as ascorbic acid in the composition of CS (Rahman and Rosli, 2014) CS can also act as a reducing agent (Kumar et al., 2020).

Click chemistry first was reported by Sharples in 2001, to describe an effective method for the synthesis of various compounds especially various pharmaceuticals. One of the most

important categories of click reactions is the CuAAC reaction between terminal alkynes and azides in the presence of a copper catalyst(I) to form 1,4-disubstituted 1,2,3-triazoles (Kolb et al., 2001; Bahsis et al., 2018; Finn and Fokin, 2010; Wang et al., 2015) that have applications in the various fields such as pharmaceutical industry, dyes, agriculture, corrosion inhibitors, optical brighteners and biological activity like hypotensive medications, anti-tuberculosis, anti-allergic, anti-bacterial, anti-HIV and Src-kinase inhibitors (Zirak and Garegeshlagi, 2018; Vibhute et al., 2018; Aghbash et al., 2019; Pagliai et al., 2006; Dolatkahh et al., 2018; Choi et al., 2020). Several example of 1,2,3-triazole compounds have anticancer property such as carboxy amido triazole (CAI), *tert*-butyl dimethyl silyl spiroamino oxathiole dioxide(TSAO), β -lactum antibiotic Tazobactam and Cefatrizine (Fig. 1) (Agalave et al., 2011; Mohammadi et al., 2018).

Considerable research has focused on using bio-based materials to reduce costs, create cost-effective and environmentally friendly materials, and numerous reports have documented the use of natural compounds as catalysts. Among the reports on the use of natural substances as catalyst for triazoles synthesis, the use of CeI/Cu (Hamzavi et al., 2020), CuICC (Ghosh et al., 2020), GO-Fe₃O₄@CuO (Jain et al., 2020), L-Proline-MCM-41-CuCl (Zhao et al., 2020), γ -Fe₂O₃@Sh@Cu₂O (Norouzi and Javanshir, 2020), Whey protein (Garg et al., 2021), CuBr/[DBU]OAc (Garg et al., 2020) and Cu₂O@PS (Dolatkahh et al., 2019) can be pointed out. These documents, along with articles which use magnetic core as based of the heterogeneous catalyst, emphasize on the easier use and green synthesis procedure (Hassankhani et al., 2021; Nourmohammadi et al., 2021). All these issues led us to design a project in which CS bio-waste was used as a support and reducing agent to prepare CS@Cu₂O and Fe₃O₄@SiO₂-pAMBA-CS-Cu₂O as heterogeneous catalysts for the synthesis of triazole derivatives



Scheme 1 Graphical scheme of the reaction.

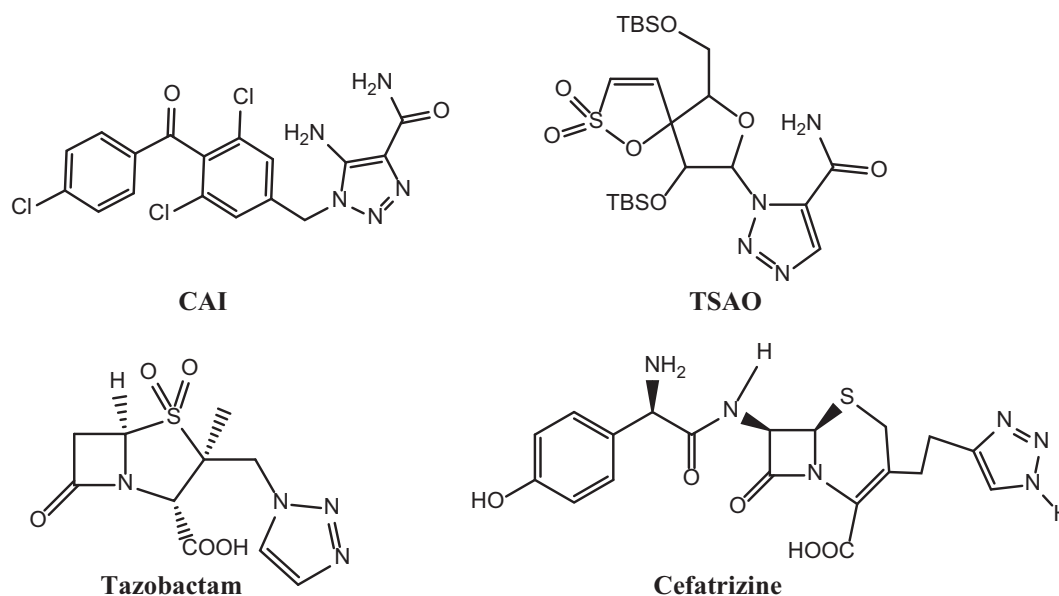


Fig. 1 Anticancer compounds containing 1, 2, 3-triazole.

2. Methods

2.1. Materials

All chemicals were purchased from Merck, Aldrich or Fluka were used without further purification. All of them were analytical grade. Fourier-transform infrared (FT-IR) spectroscopy spectra were recorded in KBr on Bruker FT-IR spectrometer and are reported in wave numbers (cm^{-1}). All melting points were measured on a capillary melting point apparatus.¹H NMR spectra were performed by a Bruker Avance DPX 300. Scanning electron microscopy (SEM) was recorded on a VEG//TESCAN 100EM10C-KV and transmission electron microscopy (TEM) was recorded on a Zeiss EM900. The surface area of catalyst was recorded Brunauer-Emmett-Teller (BET) Surface Area & Porosity Analyzer. Energy-dispersive X-ray (EDX) spectroscopy was recorded on a VEG//TESCAN-XMU. X-ray diffraction (XRD) pattern was recorded on a Bruker AXS D8-advance X-ray diffractometer using Cu K α radiation ($\lambda = 1.5418\text{\AA}$). Magnetic measurements were performed using a vibrating sample magnetometer (VSM) analysis. The metal loading was detected by an inductively coupled plasma-atomic emission spectrometer (ICP).

X-ray photoelectron spectroscopy (XPS) spectra are obtained using the Thermofisher Scientific K-Alpha XPS spectrometer. Thermal Gravimetric Analysis (TGA) and Differential Thermogravimetric (DTG) were recorded on a STA 504 BÄHR Thermoanalyse GmbH (Hüllhorst, Germany).

2.2. Preparation of CS@Cu₂O

The collected corn silks were washed with distilled water several times to remove impurities, dried in an oven at 60 °C, and powdered in a ball-mill. The ball-milled CS (1 g) and EtOH (30 mL) were mixed in a round-bottom flask and stirred at room temperature for 30 min. Then 0.5 g of Cu(OAc)₂ was added to the mixture under vigorous stirring for overnight.

The catalyst was then centrifuged and washed with water, ethanol, and acetone and dried in the oven at 70 °C.

2.3. Preparation of Fe₃O₄ nanoparticles

Fe₃O₄ nanoparticles was synthesized according to our previous method (Dolatkhah et al., 2018). In a typical procedure, a solution with a 2:1 ratio of Fe²⁺/Fe³⁺ from FeCl₂·4H₂O and FeCl₃·6H₂O in deionized water was prepared. After 2 h of stirring under N₂ atmosphere, the participation was performed by dropwise addition of NaOH solution (1 M) until pH was adjusted to 10. The magnetic nanoparticle was separated by an external magnetic field, then washed three times with deionized water and ethanol. Eventually, Fe₃O₄ particles dried for 10 h in an oven at 65 °C.

2.4. Preparation of Fe₃O₄@SiO₂-pAMBA-CS-Cu₂O

First, 1 g of Fe₃O₄ magnetite in 50 mL of water were added in a round-bottom flask and stirred at room temperature for 30 min. Then, 5 mL of ammonia solution and 50 mL EtOH was added to the mixture. In the next step, a mixture of 1.5 mL TEOS and 10 mL ethanol was added into the suspension drop by drop under vigorous stirring for 24 h. The obtained precipitate Fe₃O₄@SiO₂ was collected with a magnet, washed several times with H₂O and EtOH and dried.

1 g of Fe₃O₄@SiO₂ in 100 mL of water were dissolved in a round-bottom flask. Then, 0.3 g of *para*-aminomethyl benzoic acid was added to the mixture. The mixture was stirred vigorously for 12 h under reflux conditions the obtained precipitate Fe₃O₄@SiO₂-pAMBA was Exit with a magnet, washed with H₂O and EtOH and dried at 50 °C.

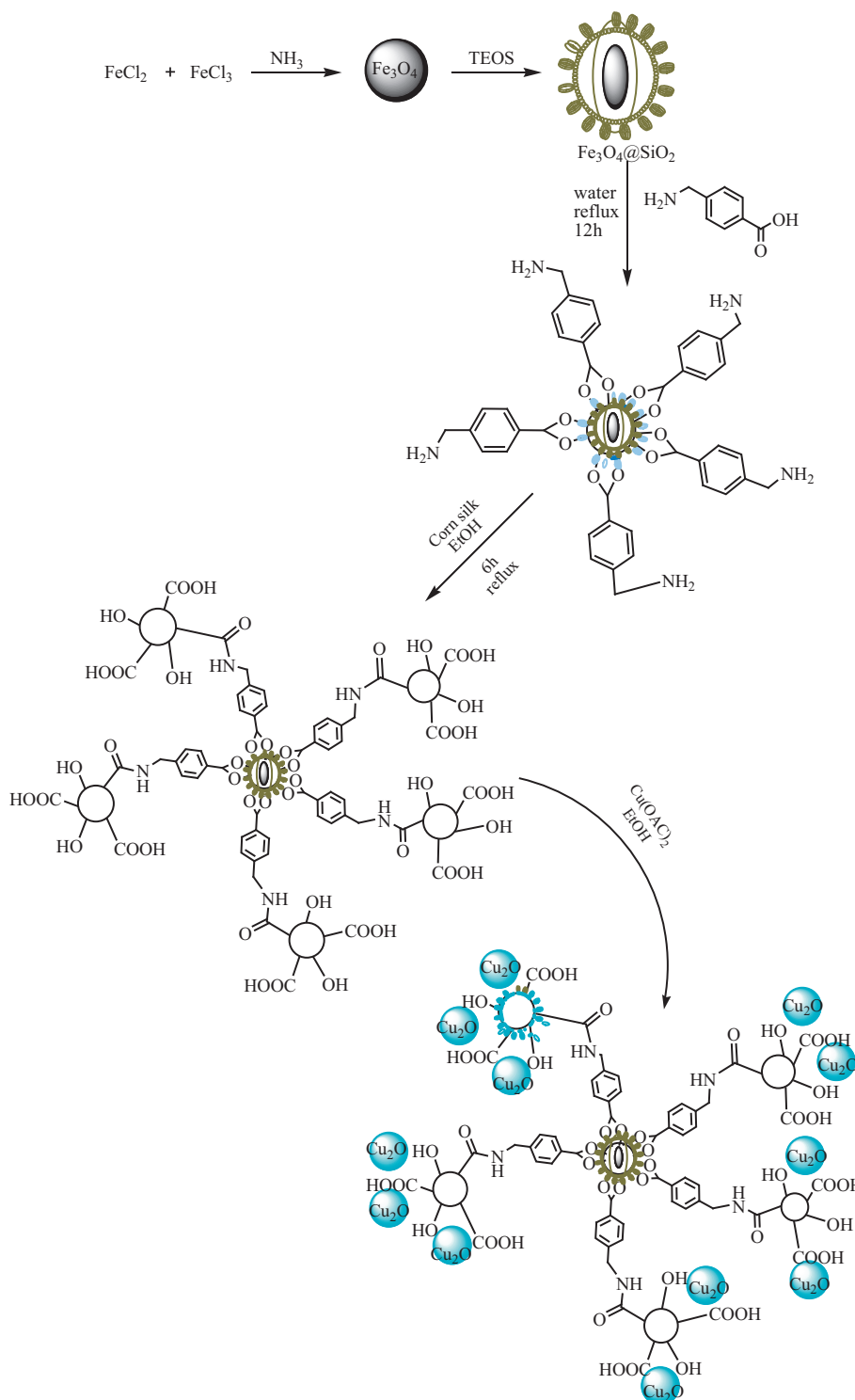
1 g of Fe₃O₄@SiO₂-pAMBA in 50 mL of EtOH were mixed for 30 min at room temperature. Then, 0.2 g of powder CS was added to the mixture and the mixture was stirred vigorously for 6 h under reflux conditions. Finally, the obtained precipitate Fe₃O₄@SiO₂-pAMBA-CS was magnetically separated,

washed several times with H₂O and EtOH and dried at 50 °C for 12 h.

1 g of Fe₃O₄@SiO₂-pAMBA-CS in 30 mL of EtOH were dispersed in a round-bottom flask and stirred at room temperature for 30 min. Then, 0.5 g of Cu(OAc)₂ was added to the mixture under vigorous stirring for overnight (Scheme 2). The final catalyst was washed with distilled water, then dried at room temperature.

2.5. General procedure for click reactions

NaN₃ (1.2 mmol), alkyne (1.2 mmol) and benzyl halide (1 mmol) were added to a suspension of CS@Cu₂O (7 mol% Cu, 0.05 g catalyst) or Fe₃O₄@SiO₂-pAMBA-CS-Cu₂O (7 mol% Cu, 0.06 g catalyst) in H₂O (2 mL). The reaction mixture was stirred at 70 °C and monitored by TLC (EtOAc:n-hexane (1:5)). After completion of the reaction, the catalyst



Scheme 2 Synthesis of Fe₃O₄@SiO₂-pAMBA-CS-Cu₂O.

was easily removed from reaction mixture and the filtrate was extracted with chloroform (2×2 mL). The organic solvents were removed under vacuum and the pure product was obtained by recrystallization with CHCl₃: n-hexane (1:3). All of the Click products are known compound and were reported previously.

3. Results and discussions

3.1. Characterization of the catalyst

The catalysts were characterized by diverse physicochemical techniques such as FT-IR, XRD, SEM, TEM, EDX, VSM, BET, XPS and ICP.

3.1.1. FT-IR investigation

The FT-IR spectra of CS, CS@Cu₂O, and recycled CS@Cu₂O after five runs in click reaction are shown in Fig. 2. The wide peak at 3400 cm⁻¹ indicates the presence of an acidic group in the CS. The peaks around 1654 cm⁻¹ and 1049 cm⁻¹ belongs to C=O and C—O bond respectively. The slight shift from 1654 cm⁻¹ in CS to 1643 cm⁻¹ in CS@Cu₂O may be due to the chelation of copper on the surface of CS.

The FT-IR spectra of Fe₃O₄, Fe₃O₄@SiO₂, Fe₃O₄@SiO₂-pAMBA-CS, Fe₃O₄@SiO₂-pAMBA-CS-Cu₂O and recycled Fe₃O₄@SiO₂-pAMBA-CS-Cu₂O after five runs are shown in Fig. 3. The FT-IR spectrum of Fe₃O₄ displays an intense absorption band at 588 cm⁻¹ attributed to the typical Fe—O vibrations of the magnetite structure whereas a broad band

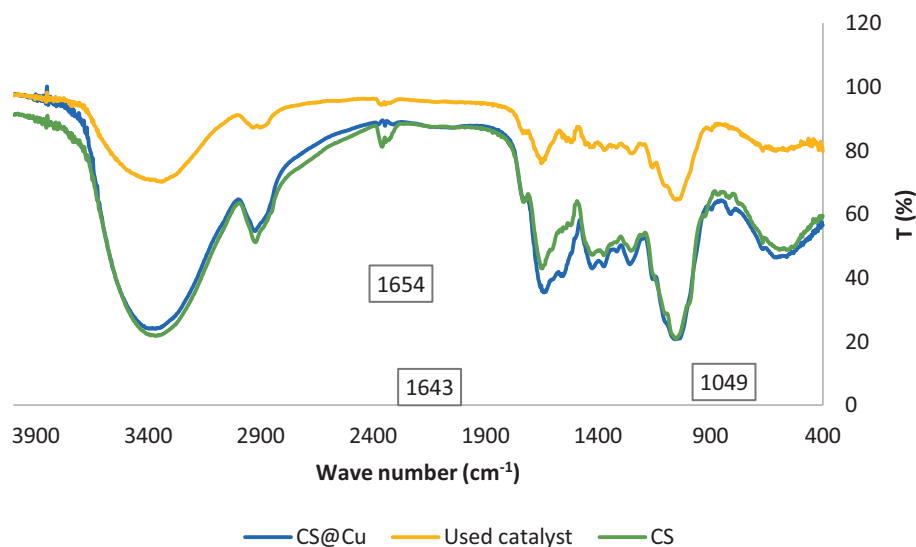


Fig 2 FT-IR spectra of CS (a), CS@Cu₂O (b), CS@Cu₂O after 5 times use (c).

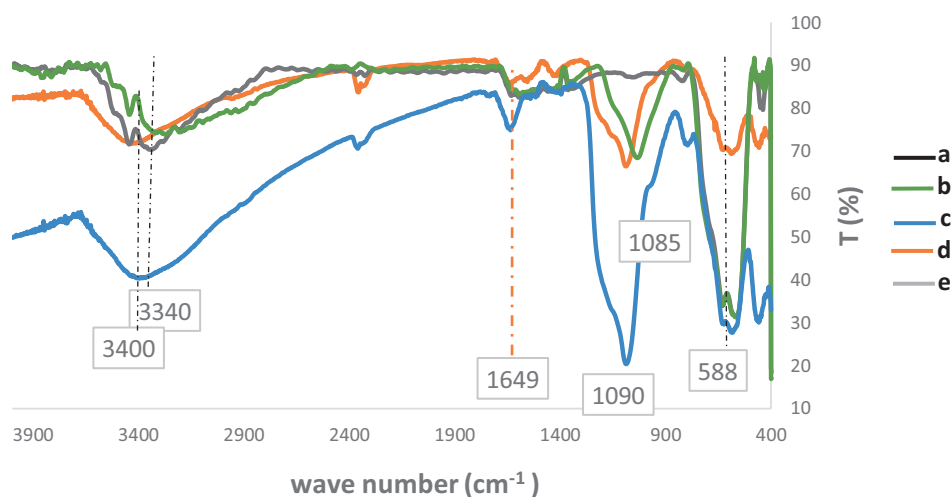


Fig 3 FT-IR spectra of Fe₃O₄ (a), Fe₃O₄@SiO₂ (b), Fe₃O₄@SiO₂-pAMBA-CS (c), Fe₃O₄@SiO₂-pAMBA-CS-Cu₂O (d), Fe₃O₄@SiO₂-pAMBA-CS-Cu₂O after 5 run in click reaction (e).

at 3340 cm^{-1} is relevant to the surface OH groups. The absorption band appeared at 1030 cm^{-1} in $\text{Fe}_3\text{O}_4@/\text{SiO}_2$ structure can be attributed to Si-O (Zandipak et al., 2020). The wide peak at around 3400 cm^{-1} indicates the presence of acidic group in the magnetic CS. The bands at 1654 cm^{-1} in the IR spectrum of $\text{Fe}_3\text{O}_4@/\text{SiO}_2\text{-pAMBA-CS-Cu}_2\text{O}$ were assigned to carbonyl groups. The slight shift from 1090 cm^{-1} in $\text{Fe}_3\text{O}_4@/\text{SiO}_2\text{-pAMBA-CS-Cu}_2\text{O}$ to 1085 cm^{-1} in $\text{Fe}_3\text{O}_4@/\text{SiO}_2\text{-pAMBA-CS-Cu}_2\text{O}$ may be due to the chelated-copper on the surface of $\text{Fe}_3\text{O}_4@/\text{SiO}_2\text{-pAMBA-CS}$.

3.1.2. Morphology study

The XRD pattern of the $\text{CS}@/\text{Cu}_2\text{O}$ shown in Fig. 4a exhibited a diffraction peak at $2\theta = 20^\circ$, which revealed the formation of amorphous copper oxide (Faeghi et al., 2018). The diffraction peak under $2\theta = 30^\circ$ belongs to CS which is amorphous organic material (Wang et al., 2014; Norouzi and Javanshir, 2020).

In the XRD pattern of the $\text{Fe}_3\text{O}_4@/\text{SiO}_2\text{-pAMBA-CS-Cu}_2\text{O}$, the diffractions at $2\theta = 35.6^\circ$, 43.3° , 62.7° , and 74.8° can be assigned to the (111), (200), (220) and (311) lattice

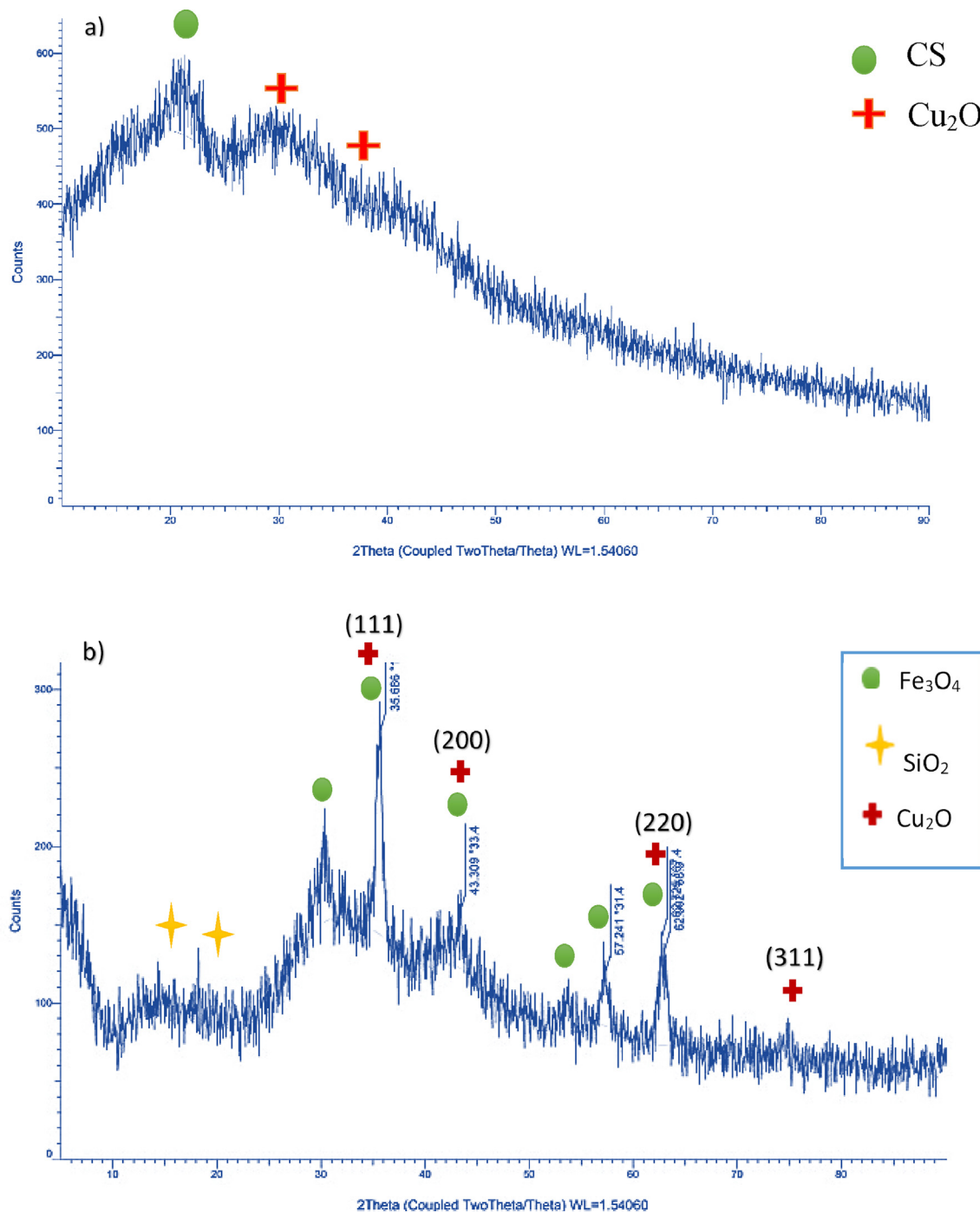


Fig 4 XRD pattern of $\text{CS}@/\text{Cu}_2\text{O}$ (a), $\text{Fe}_3\text{O}_4@/\text{SiO}_2\text{-pAMBA-CS-Cu}_2\text{O}$ (b).

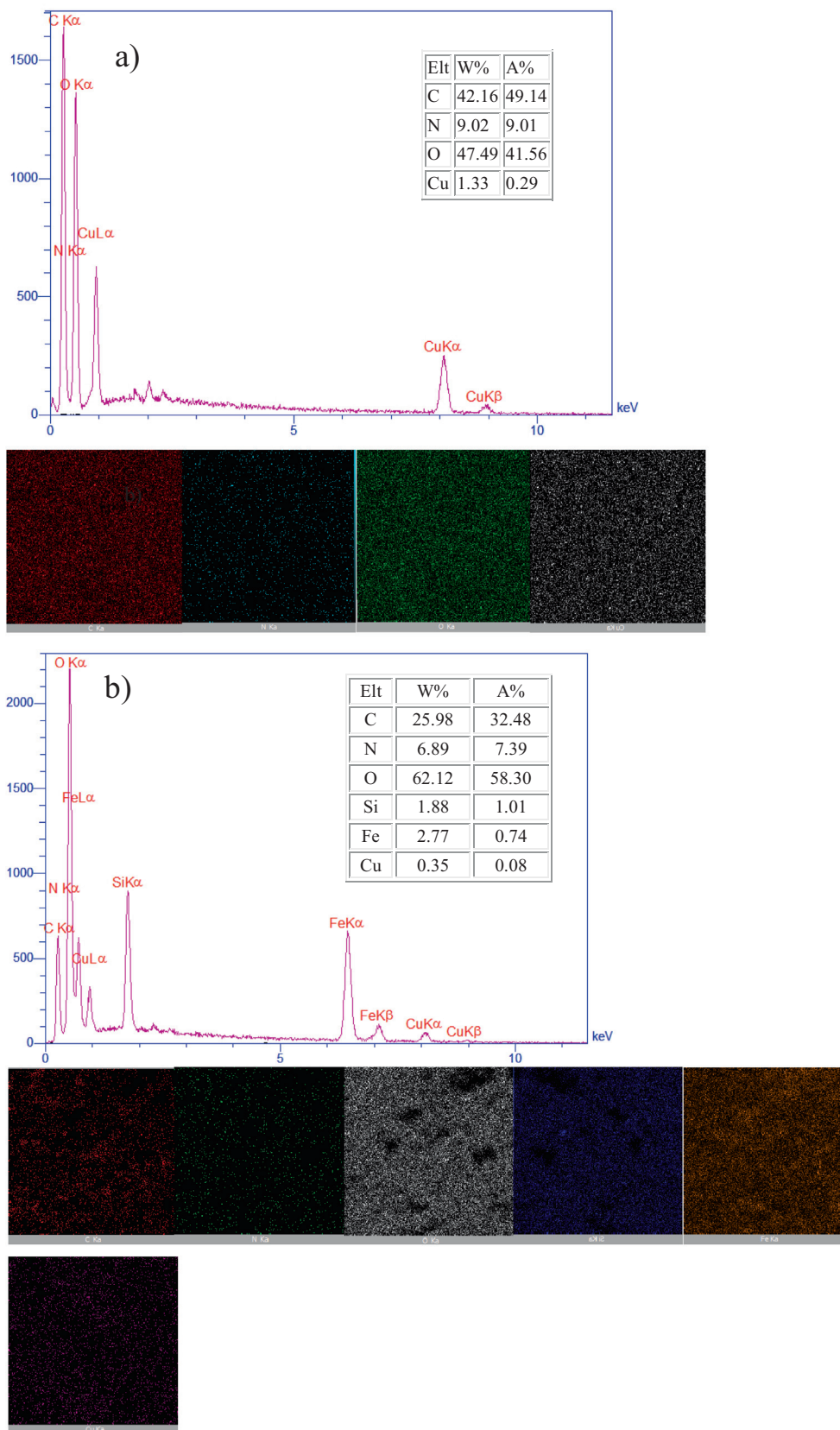


Fig 5 EDX and map analysis of CS@Cu₂O (a), Fe₃O₄@SiO₂-pAMBA-CS-Cu₂O (b). The morphology and size of Fe₃O₄, Fe₃O₄@SiO₂, Fe₃O₄@SiO₂-pAMBA-CS, Fe₃O₄@SiO₂-pAMBA-CS-Cu₂O and CS@Cu₂O NPs were investigated using SEM analysis (Fig. 6a–e). The SEM images of Fe₃O₄@SiO₂-pAMBA-CS-Cu₂O show the formation of spherical particles in size around 38–56 nm (Fig. 6d).

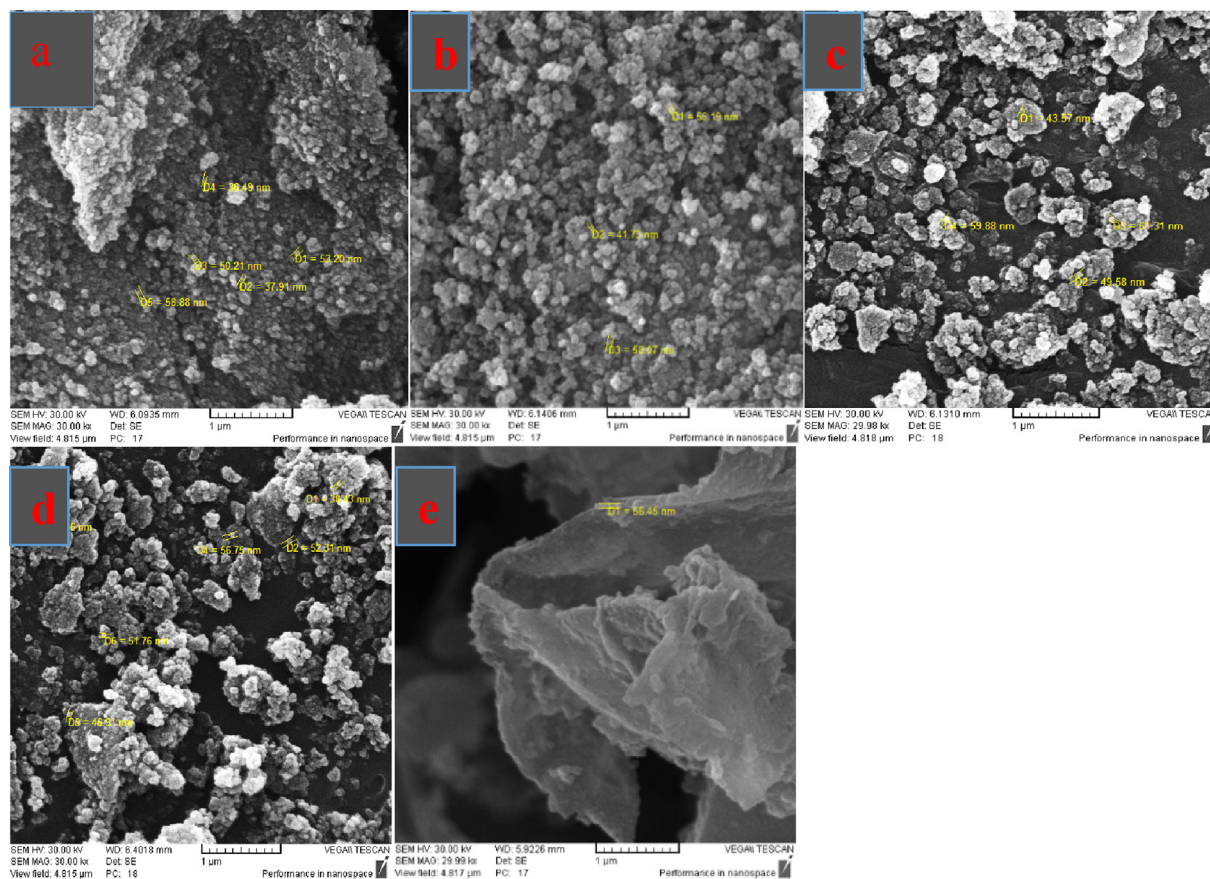


Fig 6 SEM images of Fe_3O_4 (a), $\text{Fe}_3\text{O}_4@SiO_2$ (b), $\text{Fe}_3\text{O}_4@SiO_2$ -pAMBA-CS (c), $\text{Fe}_3\text{O}_4@SiO_2$ -pAMBA-CS- Cu_2O (d), CS@ Cu_2O (e).

planes of Cu_2O , in accordance with Cu_2O standard data (JCPDS card NO. 05–0667). The diffractions at $2\theta = 30.3^\circ$, 35.6° , 43.3° , 53° , 57.1° and 62.9° can be assigned to the (220), (311), (400), (422), (511) and (440) crystalline planes of cubic lattices structure of Fe_3O_4 respectively (JCPDS No. 85–1436). Also, the peaks at around $2\theta = 14.4$ and 18.2° in the XRD pattern is due to the amorphous silica shell on the surface of the magnetite nanoparticles. (Fig. 4b).

Comparing the EDX analysis of CS@ Cu_2O clearly shows the presence of Cu, C, O and N elements in the structure of this material (Fig. 5a). Also, the presence of Cu, C, O, N, Fe and Si elements in the catalyst structure have been confirmed from the EDX analysis of $\text{Fe}_3\text{O}_4@SiO_2$ -pAMBA-CS- Cu_2O (Fig. 5b).

The TEM image of the prepared CS@ Cu_2O is shown in Fig. 7a and b. The TEM images shown two regions with different size and electron density which are related to CS@ Cu_2O nanoparticles and Cu.

The TEM image of the prepared nano- $\text{Fe}_3\text{O}_4@SiO_2$ -pAMBA-CS- Cu_2O is shown in Fig. 7c, and d. The TEM image shows the presence of three regions with different size and electron density which dense regions represent to $\text{Fe}_3\text{O}_4@SiO_2$ nanoparticles and Cu and a less dense region related to Natural base of CS (Sabaqian et al., 2017).

3.1.3. Magnetic properties

The magnetic properties of Fe_3O_4 , $\text{Fe}_3\text{O}_4@SiO_2$, $\text{Fe}_3\text{O}_4@SiO_2$ -pAMBA-CS and $\text{Fe}_3\text{O}_4@SiO_2$ -pAMBA-CS- Cu_2O were investigated using VSM analysis. The magnetization curves

recorded at room temperature are shown in Fig. 8. The saturation magnetization of Fe_3O_4 , $\text{Fe}_3\text{O}_4@SiO_2$, $\text{Fe}_3\text{O}_4@SiO_2$ -pAMBA-CS and $\text{Fe}_3\text{O}_4@SiO_2$ -pAMBA-CS- Cu_2O are 63.9, 61.49, 57.76 and 50.35 $\text{emu}\cdot\text{g}^{-1}$, respectively. The catalyst has a good magnetic property and is easily removed using an external magnet after the reaction.

3.1.4. Adsorption study

The surface area and pore volume of synthesized catalysis were estimated from the N_2 adsorption/desorption isotherms and T-plot (Fig. 9). The BET surface area and average pore diameter are $39.54\text{ m}^2\cdot\text{g}^{-1}$ and 7.17 nm for CS@ Cu_2O , and $33.65\text{ m}^2\cdot\text{g}^{-1}$ and 17.59 nm for $\text{Fe}_3\text{O}_4@SiO_2$ -pAMBA-CS- Cu_2O , respectively. The volume of the single-point adsorption cavity is $0.07\text{ cm}^3\cdot\text{g}^{-1}$ and $0.148\text{ cm}^3\cdot\text{g}^{-1}$ for CS@ Cu_2O and $\text{Fe}_3\text{O}_4@SiO_2$ -pAMBA-CS- Cu_2O , respectively. Also, the single-point cavity dissipation volume is $0.073\text{ cm}^3\cdot\text{g}^{-1}$ and $0.128\text{ cm}^3\cdot\text{g}^{-1}$ for CS@ Cu_2O and $\text{Fe}_3\text{O}_4@SiO_2$ -pAMBA-CS- Cu_2O .

In addition, as determined by ICP, the copper loading of CS@ Cu_2O and $\text{Fe}_3\text{O}_4@SiO_2$ -pAMBA-CS- Cu_2O are 1.41 and 1.25 $\text{mmol}\cdot\text{g}^{-1}$, respectively.

3.1.5. XPS analysis

To determine the oxidation states of Cu in the prepared nanocomposite, XPS analysis was performed and the obtained results are depicted in Fig. S1. The Fine-scan XPS spectrum (Fig. S1a) demonstrates that $\text{Fe}_3\text{O}_4@SiO_2$ -pAMBA-CS-

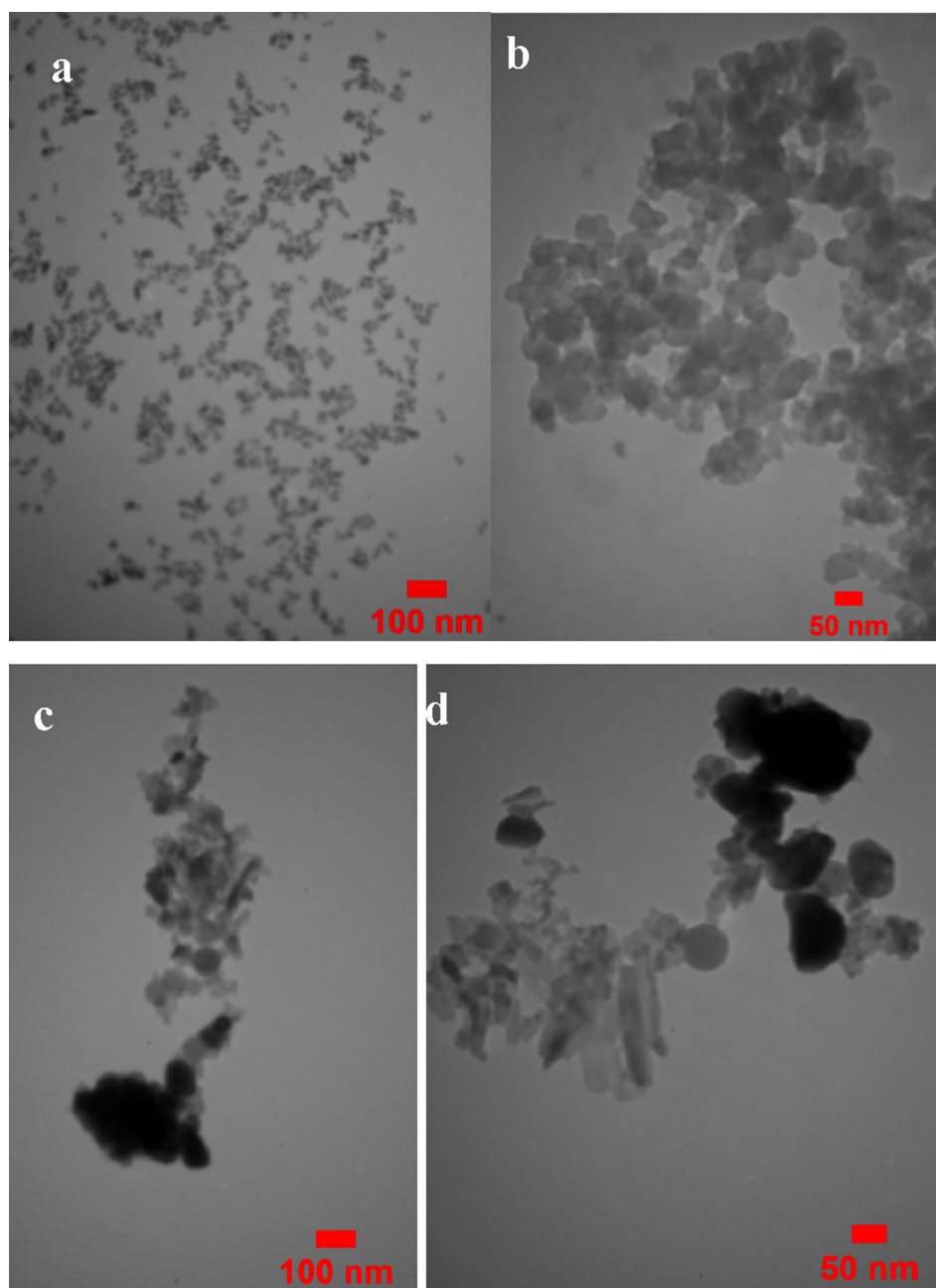


Fig 7 TEM images of CS@Cu₂O (a, b), Fe₃O₄@SiO₂-pAMBA-CS-Cu₂O (c, d).

Cu₂O contains Fe, Cu, O, Si and C elements. The peaks at around 104.5 eV in Fig. S1a correspond to SiO₂ (Jensen et al., 2013). The high-resolution spectrum of Fe 2p shown in Fig. S1b exhibited two main peaks of Fe 2p_{3/2} at around 710.8 and 714.1 eV attributed to Fe²⁺ and Fe³⁺, respectively, demonstrating the existence of Fe₃O₄. The peak at 724.6 eV, corresponding to Fe 2p_{1/2} is also in accordance with the reported values for Fe₃O₄ (Huang et al., 2017). The characteristic peaks at 932.7 and 943.80 corresponding to Cu 2p_{3/2} and Cu 2p_{1/2}, respectively, demonstrate the existence of Cu₂O (Vasquez, 1998).

3.1.6. TGA analysis

The thermal behavior of the catalyst was determined by TGA and DTG (Fig. S2). The TGA thermogram of Fe₃O₄@SiO₂-pAMBA-CS-Cu₂O shows two step weight loss steps over the temperature range of TG analysis. The first step, including a low amount of weight loss (5%) at T ~ 120 °C, resulted from the release of both the physisorbed and chemisorbed water, the second stage at about 280 °C to nearly 450 °C is attributed to the decomposition of the organic moiety in the nanocomposite including a weight loss (40%). The amount of organic compounds bound on the surface of the nanoparticles is pre-

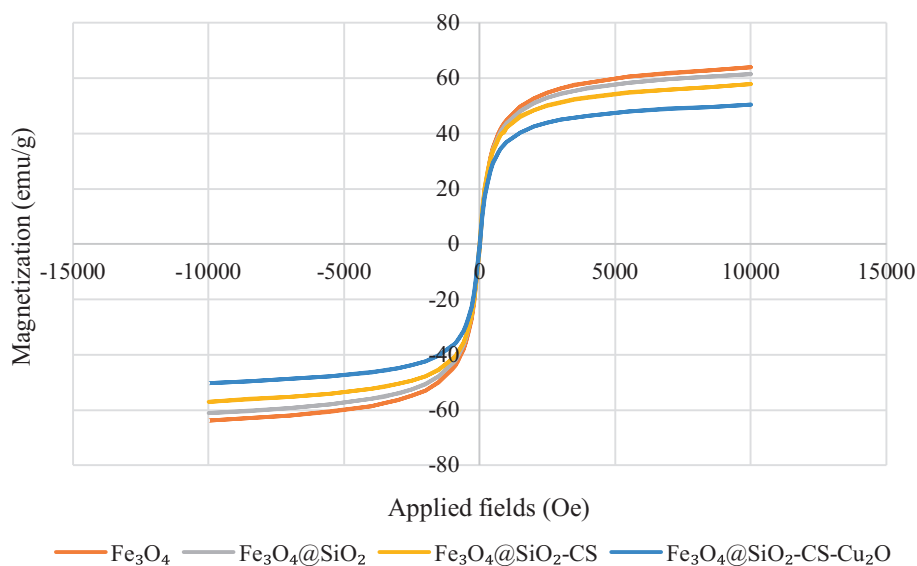


Fig 8 VSM analysis for Fe_3O_4 (a), $\text{Fe}_3\text{O}_4@\text{SiO}_2$ (b), $\text{Fe}_3\text{O}_4@\text{SiO}_2\text{-pAMBA-CS}$ (c), and $\text{Fe}_3\text{O}_4@\text{SiO}_2\text{-pAMBA-CS-Cu}_2\text{O}$ (d).

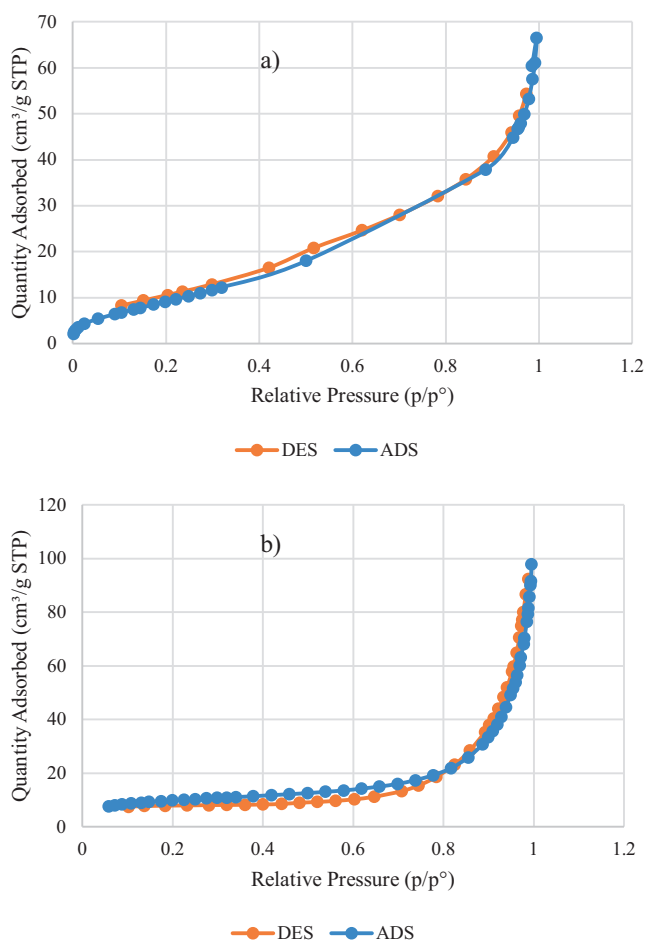


Fig 9 BET analysis of $\text{CS}@\text{Cu}_2\text{O}$ (a), $\text{Fe}_3\text{O}_4@\text{SiO}_2\text{-pAMBA-CS-Cu}_2\text{O}$ (b).

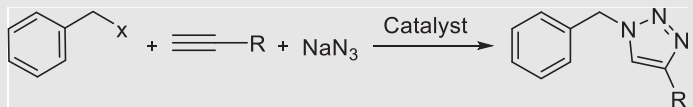
dictable from the percentage of weight loss from the TGA curve.

3.2. Catalytic studies

The catalytic behavior of $\text{CS}@\text{Cu}_2\text{O}$ and $\text{Fe}_3\text{O}_4@\text{SiO}_2\text{-pAMBA-CS-Cu}_2\text{O}$ were investigated in the click synthesis of 1,2,3-triazoles. The reaction of benzyl bromide, sodium azide and phenyl acetylene approved as a model reaction for carrying out in different conditions. The results are shown in Table 1 (Entries 1–18). This reaction was done by employing various solvents such as EtOH, toluene, EtOH- H_2O , chloroform and H_2O at 70 °C for 1 h (Entries 1–7). It was found that H_2O was the most effective solvent for triazole synthesis. Then, other conditions like temperature, amount of catalyst and presence/absence of the base was examined in the model reaction (Entries 9–17). It was found that by increasing the amount of $\text{CS}@\text{Cu}_2\text{O}$ and $\text{Fe}_3\text{O}_4@\text{SiO}_2\text{-pAMBA-CS-Cu}_2\text{O}$ from 0.5 to 7 mol%, the yield increased from 74% to 96%, and 69% to 93% respectively (Table 1, Entries 12–16). Further increase in catalyst amount had no profound effect on the yield of the desired product. The reaction has not progressed in the absence of catalyst (Entry 18). Accordingly, the best results are obtained when the reaction is performed in water in the presence of 7 mol% of the both catalysts at 70 °C (Table 1, Entry 16). Some of the catalyst components such as Fe_3O_4 , $\text{Fe}_3\text{O}_4@\text{SiO}_2$, $\text{Fe}_3\text{O}_4@\text{SiO}_2\text{-pAMBA-CS}$, CS, and $\text{Cu}(\text{OAc})_2$ were also examined under optimal conditions. However, in most cases the reaction efficiency was not improved (Table 2).

Subsequently, the reaction among various benzyl halide derivatives, acetylene derivatives and NaN_3 was investigated and the corresponding triazoles were obtained in good to excellent yields within relatively short times (Table 3).

The catalytic activity of $\text{CS}@\text{Cu}_2\text{O}$ and $\text{Fe}_3\text{O}_4@\text{SiO}_2\text{-pAMBA-CS-Cu}_2\text{O}$ were compared with other catalysts in the Click reaction of phenylacetylene, benzyl bromide and NaN_3

Table 1 Optimize the reactions condition synthesis of 1-benzyl-4-phenyl-1*H*-1,2,3-triazole using catalyst^a.


Entry	Solvent	T(°C)	Base	Cat. (mol%)	Isolated yield (%) ^[b]	Isolated yield (%) ^[c]
1	EtOH	70	K ₂ CO ₃	5	71	69
2	Toluene	70	K ₂ CO ₃	5	Trace	Trace
3	H ₂ O:EtOH (1:1)	70	K ₂ CO ₃	5	84	79
4	H ₂ O:EtOH (2:1)	70	K ₂ CO ₃	5	62	52
5	H ₂ O:EtOH (1:2)	70	K ₂ CO ₃	5	76	69
6	Chloroform	70	K ₂ CO ₃	5	Trace	Trace
7	H ₂ O	70	K ₂ CO ₃	5	87	82
8	H ₂ O	70	—	5	88	85
9	H ₂ O	25	—	5	58	55
10	H ₂ O	50	—	5	63	59
11	H ₂ O	70	—	5	88	85
12	H ₂ O	70	—	0.5	74	69
13	H ₂ O	70	—	1	80	72
14	H ₂ O	70	—	2.5	84	78
15	H ₂ O	70	—	5	88	85
16	H ₂ O	70	—	7	96	93
17	H ₂ O	70	—	10	96	93
18	H ₂ O	70	K ₂ CO ₃	—	Trace	Trace

^a Reaction conditions: benzyl bromide (1 mmol), sodium azide (1.1 mmol), phenylacetylene (1 mmol) and catalyst (7 mol%) in water at 70 °C,

^b Catalyst = CS@Cu₂O, ^c Catalyst = Fe₃O₄@SiO₂-pAMBA-CS-Cu₂O.

Table 2 Screening catalysts for the three-component reaction of benzyl bromide, sodium azide and phenyl acetylene.

Entry	Catalyst	Time	Isolated yield
1	Fe ₃ O ₄	360 min	—
2	Fe ₃ O ₄ @SiO ₂	360 min	—
3	Fe ₃ O ₄ @SiO ₂ -CS	360 min	—
4	CS	360 min	Trace
5	Cu(OAc) ₂	360 min	Trace
6	CS@Cu ₂ O	20 min	96
7	Fe ₃ O ₄ @SiO ₂ -pAMBA-CS-Cu ₂ O	20 min	93

(Table 4). The use of H₂O as green solvent and natural base catalyst, easy isolation of product from the reaction mixture, absence of reducing agent and base, operational simplicity, high yield and reusability of catalyst are the merits of present method.

Then, we examined the heterogeneous nature of the catalysts. The catalytically active particles were removed from the reaction by filtration after 5 min using a hot filtration. The reaction progress did not change after running the hot filtration (Fig. 10a, b).

The reusability of catalysts was investigated in the reaction of benzyl bromide, phenylacetylene, and NaN₃. After comple-

tion of the reaction, the catalyst was recovered by an external magnet and washed several times with EtOH, and then re-used after drying it at 60 °C. The results show that the performance of the catalyst did not decrease significantly after recycling (Fig. 11a, b).

A mechanism for the catalytic activity in the synthesis of 1-aryl-1,2,3-triazole derivatives is shown in Scheme 3. Initially, catalyst and acetylene are joined together and then alkyl azide is added. Then, an unusual six-membered copper metallacycle is formed and finally, the catalyst is removed and triazole is formed (Wang et al., 2016) Scheme 4.

3.3. Selected characterization data

(1-(4-Methylbenzyl)-1*H*-1,2,3-triazol-4-yl) methanol (**3j**): IR (KBr): 653.7, 777.1, 835, 1012.4, 1121.8, 1222, 1330, 1446.3, 1515.7, 2944.7, 3249.4.

¹H NMR (400 MHz, CDCl₃, 25 °C, TMS): δ = 2.32 (3H, s), 2.99 (1H, s), 4.72 (2H, s), 5.44 (2H, s), 7.15 (4H, s), 7.40 (1H, s).

4. Conclusion

Herein, we reported the synthesis of two eco-friendly heterogeneous catalyst, CS@Cu₂O and Fe₃O₄@SiO₂-pAMBA-CS-Cu₂O, and their high catalytic performance for

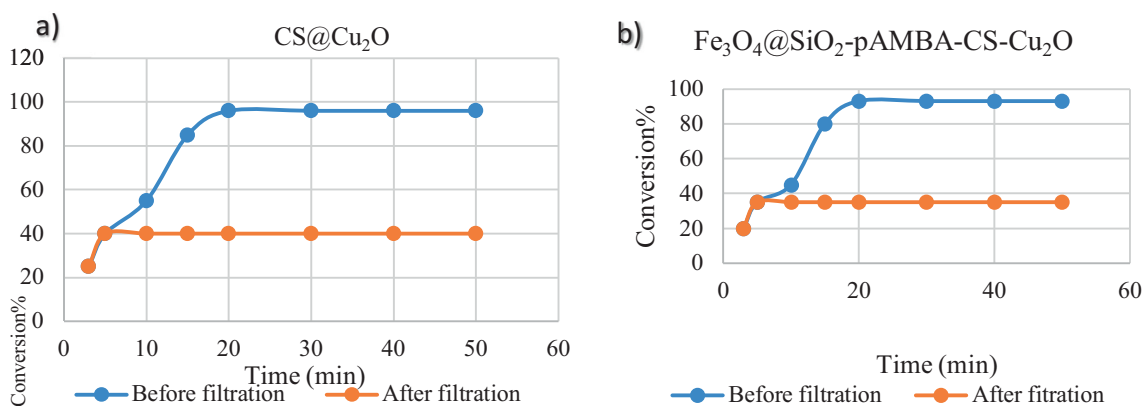
Table 3 Synthesis of 1*H*-1,2,3-triazoles using catalyst.

Entry	R ¹	R ²	X	Product	Time (min) ^[a]	Time (min) ^[b]	Isolated yield ^[a]	Isolated yield ^[b]	M.P. (°C)	Ref.
1	Ph	Ph	Br	3a	20	20	96	93	129–130	(Khalili and Rezaee, 2019)
2	Ph	Ph	Cl	3b	20	25	92	89	128–129	(Velpuri and Muralidharan, 2019)
3	Ph	4-Br-Ph	Br	3c	20	20	98	95	151–153	(Pasupuleti and Bez, 2019)
4	Ph	4-Me-Ph	Br	3d	20	20	91	89	110–112	(Bunev et al., 2016)
5	Ph	4-NO ₂ -Ph	Br	3e	25	30	89	86	155–157	(Lai et al., 2018)
6	Ph	2-Cl-Ph	Cl	3f	30	35	88	84	83–86	(Zarchi and Nazem, 2014)
7	CH ₂ OH	Ph	Br	3 g	25	30	90	90	74–76	(Khojastehnezhad et al., 2019)
8	CH ₂ OH	Ph	Cl	3 h	30	35	86	85	77–79	(Bahri-Laleh et al., 2018)
9	CH ₂ OH	4-Br-Ph	Br	3i	25	25	93	89	110–112	(Safa and Mousazadeh, 2016)
10	CH ₂ OH	4-Me-Ph	Br	3j	25	25	87	84	91–93	(Dubrovina et al., 2013)
11	CH ₂ OH	4-NO ₂ -Ph	Br	3 k	30	30	84	79	122–123	(Apperley et al., 2017)
12	CH ₂ OH	2-Cl-Ph	Cl	3 l	40	40	86	82	98–100	(Safa and Mousazadeh, 2016)

^a Reaction conditions: benzyl bromide (1 mmol), sodium azide (1.1 mmol), phenylacetylene (1.1 mmol) and catalyst (7 mol%) in water at 70 °C, ^a Cat. = CS@Cu₂O, ^b Cat. = Fe₃O₄@SiO₂-pAMBA-CS-Cu₂O.

Table 4 Comparison of efficiency of various catalysts for triazole synthesis (based on model reaction).

Entry	Catalyst	Catalyst loading	Time	T (°C)	Solvent	Yield	Refs.
1	bis-(MIM)(CuBr ₂)	5 mol%	1 h, 40 min	80	H ₂ O/EtOH	91	(Dige et al., 2017)
2	Cu(I)-AMPS	1 mol%	1 h	25	H ₂ O	82	(Bahsis et al., 2019)
3	Mag-Cu	2 mol%	6 h	55	H ₂ O/tBuOH	93	(Banan et al., 2017)
4	AA-Clin@Cu	0.06 g	24 h	25	H ₂ O	94	(Gholinejad et al., 2019)
5	Fe ₃ O ₄ @LDH@cysteine-Cu(I)	0.02 g	25 min	75	Choline azide	90	(Pazoki et al., 2020)
6	Fe ₃ O ₄ @SiO ₂ -PIA-Cu	0.01 g	12 h	70	H ₂ O	95	(Zirak and Garegeshlagi, 2018)
7	CS@Cu ₂ O	7 mol%	20 min	70	H ₂ O	96	This work
8	Fe ₃ O ₄ @SiO ₂ -pAMBA-CS-Cu ₂ O	7 mol%	20 min	70	H ₂ O	93	This work

**Fig 10** Hot filtration test of CS@Cu₂O (a), Fe₃O₄@SiO₂-pAMBA-CS-Cu₂O (b).

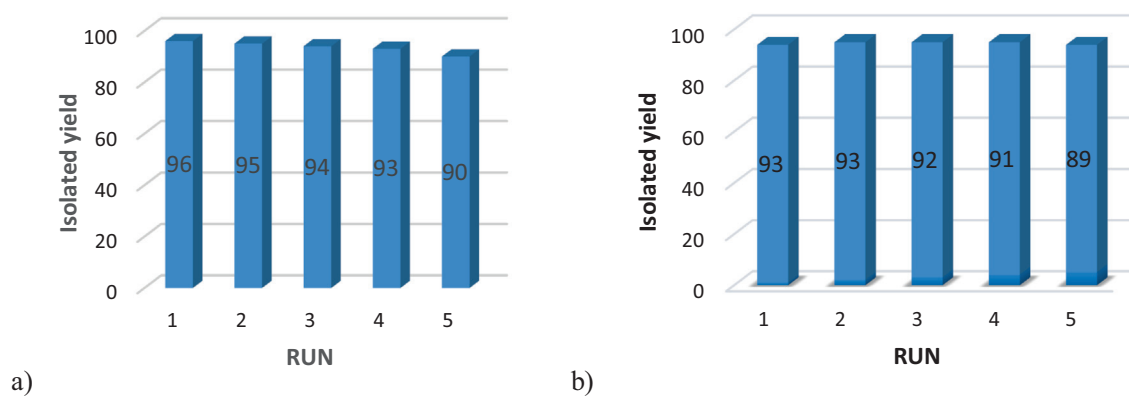
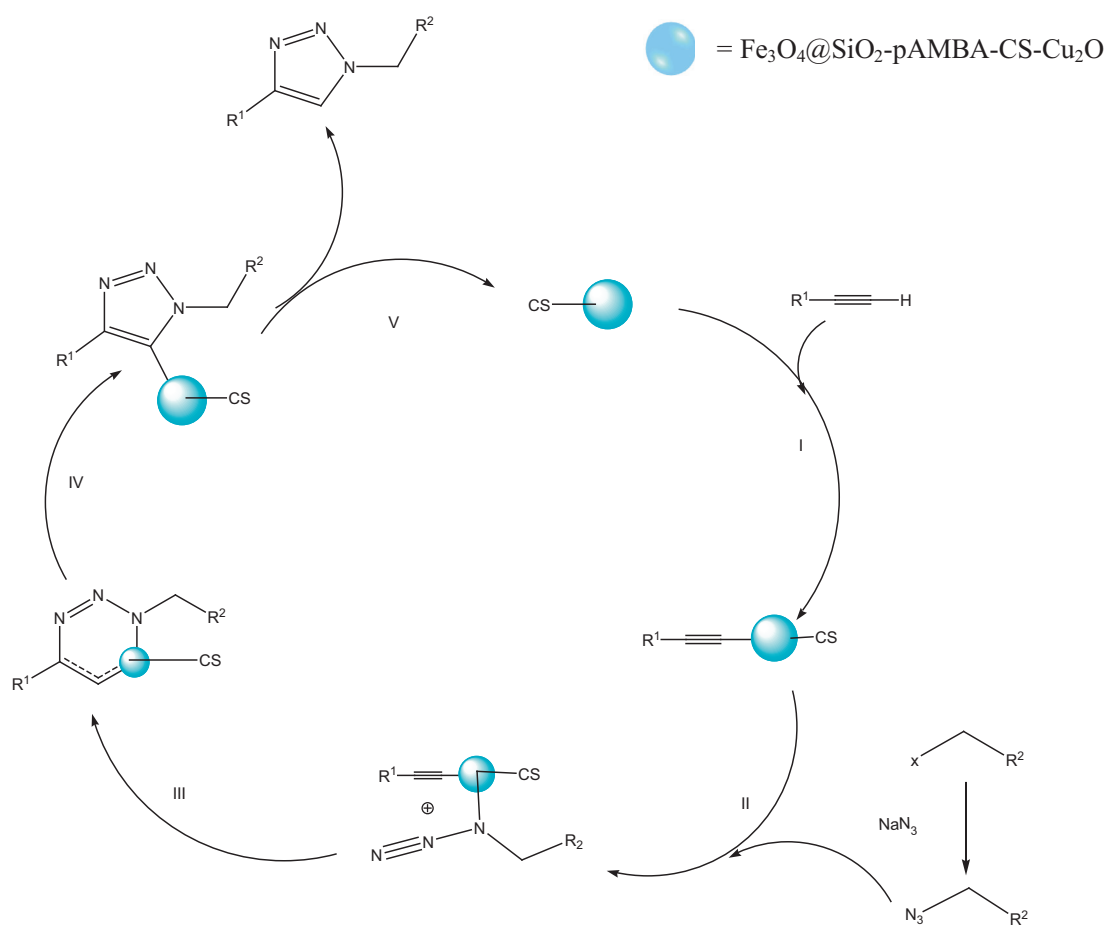


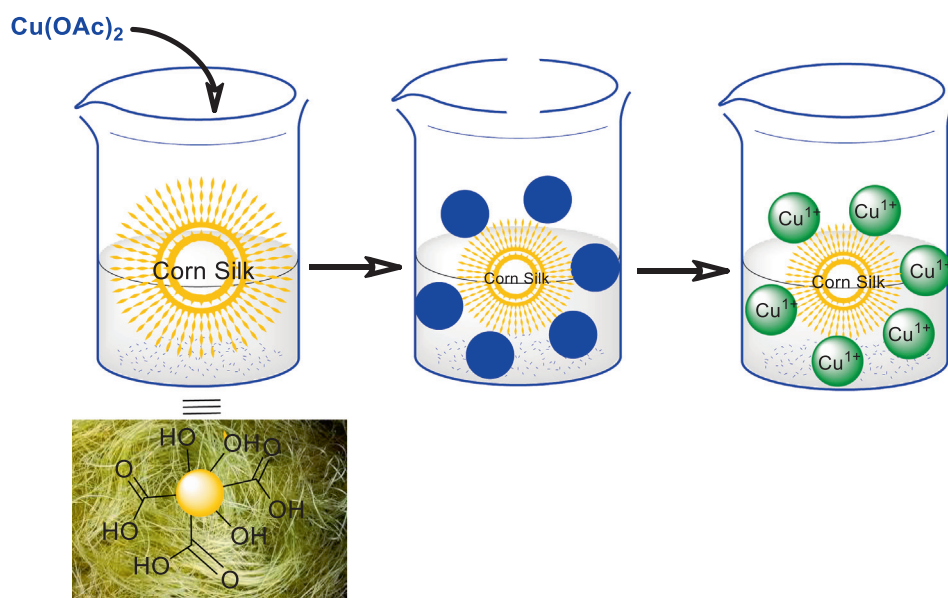
Fig 11 Recyclability of CS@Cu₂O (a), Fe₃O₄@SiO₂-pAMBA-CS-Cu₂O (b).



Scheme 3 Suggested mechanism for model reaction.

the synthesis of 1,2,3-triazole derivatives *via* a one-pot Huisgen 1,3-dipolar cycloaddition reaction in H₂O at 70 °C. The existence of natural reducing agents such as the ascorbic acid in the CS structure allows it to act as a reducing agent and convert Cu(OAc)₂ to Cu₂O.

This approach for triazoles synthesis is distinguished by the exploitation and valorisation of CS biomass waste for the preparation of a green and recyclable catalyst, its high atom economy, low catalyst loading, simple operations under mild



Scheme 4 Proposed mechanism for the generation of Cu (I).

conditions, good product yields, the ease of catalyst-product separation, alongside absence of any reducing agent and base.

Funding Source Declaration

This research did not receive any specific grant from funding agencies in the public, commercial, or not-for-profit sectors.

Declaration of Competing Interest

The authors declare that they have no known competing financial interests or personal relationships that could have appeared to influence the work reported in this paper.

Appendix A. Supplementary material

Supplementary data to this article can be found online at <https://doi.org/10.1016/j.arabjc.2022.103838>.

References

- Agalave, S.G., Maujan, S.R., Pore, V.S., 2011. Click chemistry: 1,2,3-triazoles as pharmacophores. *Chem. asian J.* 6, 2696–2718.
- Aghbash, K.O., Pesyan, N.N., Sahin, E., 2019. Cu(I)-catalyzed alkyne-azide 'click' cycloaddition (CuAAC): a clean, efficient and mild synthesis of new 1,4-disubstituted 1H-1,2,3-triazole-linked 2-amino-4,8-dihydropyrano [3,2-b] pyran-3-carbonitrile-crystal. *Res. Chem. Intermed.* 45, 2079–2094.
- Apperley, K.Y., Roy, I., Saucier, V., Burnet-Filion, N., Piscopo, S.-P., Pardin, C., Al, E., 2017. Development of new scaffolds as reversible tissue transglutaminase inhibitors, with improved potency or resistance to glutathione addition. *MedChemComm.* 8, 338–345.
- Athinarayanan, J., Periasamy, V.S., Alshatwi, A.A., 2019. Phoenix dactylifera lignocellulosic biomass as precursor for nanostructure fabrication using integrated process. *Int. J. Biol. Macromol.* 134, 1179–1186. <https://doi.org/10.1016/j.ijbiomac.2019.05.134>.
- Bahri-Laleh, N., Sadjadi, S., Heravi, M.M., Malmir, M., 2018. CuI-functionalized halloysite nanoclay as an efficient heterogeneous catalyst for promoting click reactions: Combination of experimental and computational chemistry. *Appl. Organomet. Chem.* 32, 4283.
- Bahsis, L., Ayouchia, H.B., El, Anane, H., Benhamou, K., Kaddami, H., Julve, M., Al, E., 2018. Cellulose-copper as bio-supported recyclable catalyst for the clickable azide-alkyne [3 + 2] cycloaddition reaction in water. *Int. J. Biol. Macromol.* 119, 849–856.
- Bahsis, L., El-Ayouchia, H.B., Anane, H., Pascual-Alvarez, A., Munno, G.D., Julve, M., Al, E., 2019. A reusable polymer-supported copper(I) catalyst for triazole click reaction on water: An experimental and computational study. *Appl. Organomet. Chem.* 33, 4669.
- Banan, A., Bayat, A., Valizadeh, H., 2017. Copper immobilized onto polymer-coated magnetic nanoparticles as recoverable catalyst for 'click' reaction. *Appl. Organomet. Chem.* 31, 3604.
- Buneev, A., Belinskaya, E., Gryzunova, N., Vikarchuk, A., 2016. Copper(II) oxide nanowhiskers—A new efficient catalyst of azide-alkyne cycloaddition. *Russ. J. Org. Chem.* 52, 1537–1539.
- Choi, H., Kim, M., Jang, J., Hong, S., 2020. Visible-Light-Induced Cysteine-Specific Bioconjugation: Biocompatible Thiol-Ene Click Chemistry. *Angew. Chemie* 59, 22514–22522. <https://doi.org/10.1002/ange.202010217>.
- Dige, N.C., Patil, J.D., Pore, D.M., 2017. Dicationic 1, 3-Bis (1-methyl-1H-imidazol-3-ium) propane copper(I) dibromate: novel heterogeneous catalyst for 1, 3-dipolar cycloaddition. *Catal. Letters* 147, 301–309.
- Dolatkhah, Z., Javanshir, S., Bazgir, A., Mohammadkhani, A., 2018. Magnetic Isinglass a nano-bio support for copper immobilization: Cu-IG@Fe₃O₄ a heterogeneous catalyst for triazoles synthesis. *Chemistryselect* 3, 5486–5493.
- Dolatkhah, Z., Mohammadkhani, A., Javanshir, S., Bazgir, A., 2019. Peanut shell as a green biomolecule support for anchoring Cu₂O: a biocatalyst for green synthesis of 1, 2, 3-triazoles under ultrasonic irradiation. *BMC Chem.* 13, 97.
- Dubrovina, N.V., Domke, L., Shuklov, I.A., Spannenberg, A., Franke, R., Villinger, A., Al, E., 2013. New mono-and bidentate

- P-ligands using one-pot click-chemistry: synthesis and application in Rh-catalyzed hydroformylation. *Tetrahedron* 69, 8809–8817.
- Faeghi, F., Javanshir, S., Molaei, S., 2018. Natural Polymer-Based Copper/Sandarac Resin Catalyzed Regioselective One-Pot Synthesis of 1,4-Disubstituted 1,2,3-Triazoles under Ultrasonic Irradiation.
- Finn, M., Fokin, V.V., 2010. Click chemistry: function follows form. *Chem. Soc. Rev.* 39, 1231–1232.
- Garg, A., Borah, D., Trivedi, P., Gogoi, D., Chaliha, A.K., Ali, A.A., Chetia, D., Chaturvedi, V., Sarma, D., 2020. A simple work-up-free, solvent-free approach to novel amino acid linked 1,4-disubstituted 1,2,3-triazoles as potent antituberculosis agents. *ACS Omega* 5, 29830–29837. <https://doi.org/10.1021/acsomega.0c03862>.
- Garg, A., Hazarika, R., Dutta, N., Dutta, B., Sarma, D., 2021. Bio-waste Derived Catalytic Approach Towards NH-1,2,3-Triazole Synthesis. *ChemistrySelect* 6, 7266–7270. <https://doi.org/10.1002/slct.202101347>.
- Gholinejad, M., Oftadeh, E., Sansano, J.M., 2019. Clinochlore-Supported Copper Nanoparticles as Green and Efficient Catalyst for Room-Temperature Synthesis of 1, 2, 3-Triazoles in Water. *Chemistryselect* 4, 3151–3160.
- Ghosh, D., Dhibar, S., Dey, A., Manna, P., Dey, B., 2020. A Cu(II)-inorganic Co-crystal as a versatile catalyst towards “click” chemistry for synthesis of 1,2,3-triazoles and beta-hydroxy-1,2,3-triazoles. *Chemistryselect* 5, 75–82.
- Hamzavi, S.F., Gerivani, S., Saedi, S., Naghdipari, K., Shahverdizadeh, G., 2020. preparation and characterization of a novel spherical cellulose-copper(II) oxide composite particles: as a heterogeneous catalyst for the click reaction. *Mol. Divers.* 24, 201–209.
- Hasanudin, K., Hashim, P., Mustafa, S., 2012. Corn silk (*Stigma maydis*) in healthcare: a phytochemical and pharmacological review. *Molecules* 17, 9697–9715.
- Haslina, H., Praseptianga, D., Bintoro, V.P., Pujiastanto, B., 2017. Chemical and phytochemical characteristics of local corn silk powder of three different varieties. *Int. J. Adv. Sci. Eng. Inf. Technol.* 7.
- Hassankhani, A., Gholipour, B., Rostamnia, S., Zarenezhad, E., Nouruzi, N., Kavetsky, T., Khalilov, R., Shokouhimehr, M., 2021. Sustainable design and novel synthesis of highly recyclable magnetic carbon containing aromatic sulfonic acid: Fe₃O₄@C/Ph-SO₃H as green solid acid promoted regioselective synthesis of tetrazoloquinazolines. *Appl. Organomet. Chem.* 35, 1–10. <https://doi.org/10.1002/aoc.6346>.
- Huang, M., Chen, C., Wu, S., Tian, X., 2017. Remarkable high-temperature Li-storage performance of few-layer graphene-anchored Fe₃O₄ nanocomposites as an anode. *J. Mater. Chem. A* 5, 23035–23042. <https://doi.org/10.1039/c7ta07364j>.
- Jain, Y., Kumari, M., Singh, R.P., Kumar, D., Gupta, R., 2020. Sonochemical decoration of graphene oxide with magnetic Fe₃O₄@CuO nanocomposite for efficient click synthesis of coumarin-sugar based bioconjugates and their cytotoxic activity. *Catal. Lett.* 150, 1142–1154.
- Jensen, D.S., Kanyal, S.S., Madaan, N., Vail, M.A., Dadson, A.E., Engelhard, M.H., Linford, M.R., 2013. Silicon (100)/SiO₂ by XPS. *Surf. Sci. Spectra* 20, 36–42. <https://doi.org/10.1116/11.20121101>.
- Jia, Y., Xue, Z., Wang, Y., Lu, Y., Li, R., Li, N., Wang, Q., Zhang, M., Chen, H., 2021. Chemical structure and inhibition on α -glucosidase of polysaccharides from corn silk by fractional precipitation. *Carbohydr. Polym.* 252. <https://doi.org/10.1016/j.carbpol.2020.117185>
- Sun, K., Lv, Q., Chen, X., Qu, L.B., Yu, B., 2021. Recent Advances of Visible-Light-Mediated Organic Transformations in Water. *Green Chem.* 23, 232–248. <https://doi.org/10.1039/D0GC03447A>.
- Khalili, D., Rezaee, M., 2019. Impregnated copper ferrite on mesoporous graphitic carbon nitride: An efficient and reusable catalyst for promoting ligand-free click synthesis of diverse 1, 2, 3-triazoles and tetrazoles. *Appl. Organomet. Chem.* 33, 5219.
- Khojastehnezhad, A., Bakavoli, M., Javid, A., Siuki, M.M.K., Shahidzadeh, M., 2019. Synthesis, characterization, and investigation of catalytic activity of copper(II) porphyrin graphene oxide for azide-alkyne cycloaddition. *Res. Chem. Intermed.* 45, 4473–4485.
- Kolb, H.C., Finn, M., Sharpless, K.B., 2001. Click chemistry: diverse chemical function from a few good reactions. *Angew. Chemie Int. Ed.* 40, 2004–2021.
- Kumar, B., Smita, K., Debut, A., Cumbal, L., 2020. Andean sachu inchi (*Plukenetia volubilis* L.) leaf-mediated synthesis of Cu₂O nanoparticles: A low-cost approach. *Bioengineering* 7, 1–10. <https://doi.org/10.3390/bioengineering7020054>.
- Lai, B., Mei, F., Gu, Y., 2018. Bifunctional Solid Catalyst for Organic Reactions in Water: Simultaneous Anchoring of Acetylacetonate Ligands and Amphiphilic Ionic Liquid “Tags” by Using a Dihydropyran Linker. *Chem. asian J.* 13, 2529–2542.
- Liu, J., Wang, C., Wang, Z., Zhang, C., Lu, S., Liu, J., 2011. The antioxidant and free-radical scavenging activities of extract and fractions from corn silk (*Zea mays* L.) and related flavone glycosides. *Food Chem.* 126, 261–269.
- Mohammadi, L., Zolfigol, M.A., Khazaei, A., Yarie, M., Ansari, S., Azizian, S., Al, E., 2018. Synthesis of nanomagnetic supported thiourea-copper(I) catalyst and its application in the synthesis of triazoles and benzamides. *Appl. Organomet. Chem.* 32, 3933.
- Rahman, N.A., Rosli, W.I.W., 2014. Nutritional compositions and antioxidant capacity of the silk obtained from immature and mature corn. *J. King Saud Univ.* 26, 119–127.
- Norouzi, F., Javanshir, S., 2020. Magnetic γ -Fe₂O₃@Sh@Cu₂O: an efficient solid-phase catalyst for reducing agent and base-free click synthesis of 1, 4-disubstituted-1, 2, 3-triazoles. *BMC Chem.* 14, 1–16.
- Nourmohammadi, M., Rouhani, S., Azizi, S., Maaza, M., Msagati, A. M., Rostamnia, T.S., Hatami, M., Khaksar, S., Zarenezhad, E., Jang, H.W., Shokouhimehr, M., 2021. Magnetic nanocomposite of crosslinked chitosan with 4,6-diacetylresorcinol for gold immobilization (Fe₃O₄@CS/DAR-Au) as a catalyst for an efficient one-pot synthesis of propargylamine. *Mater. Today Commun.* 29.
- Pagliai, F., Pirali, T., Grosso, E. Del, Brisco, R. Di, Tron, G.C., Sorba, G., Al, E., 2006. Rapid synthesis of triazole-modified resveratrol analogues via click chemistry. *J. Med. Chem.* 49, 467–470.
- Pasupuleti, B.G., Bez, G., 2019. CuI/L-proline catalyzed click reaction in glycerol for the synthesis of 1, 2, 3-triazoles. *Tetrahedron Lett.* 60, 142–146.
- Pazoki, F., Salamatmanesh, A., Bagheri, S., Heydari, A., 2020. Synthesis and Characterization of Copper(I)-Cysteine Complex Supported on Magnetic Layered Double Hydroxide as an Efficient and Recyclable Catalyst System for Click Chemistry Using Choline Azide as Reagent and Reaction Medium. *Catal. Letters* 150, 1186–1195.
- Ravindran, B., Karmegam, N., Yuvaraj, A., 2021. Cleaner production of agriculturally valuable benign materials from industry generated bio-wastes : A review. *Bioresour. Technol.* 320. <https://doi.org/10.1016/j.biortech.2020.124281>
- Ren, S.-C., Qiao, Q.-Q., Ding, X.-L., 2013. Antioxidative activity of five flavones glycosides from corn silk (*stigma maydis*). *Czech J. food Sci.* 31, 148–155.
- Sabaqian, S., Nemati, F., Heravi, M.M., Nahzomi, H.T., 2017. Copper (I) iodide supported on modified cellulose-based nanomagnetite composite as a biodegradable catalyst for the synthesis of 1, 2, 3-triazoles. *Appl. Organomet. Chem.* 31, 3660.
- Safa, K.D., Mousazadeh, H., 2016. Synthesis of novel 1, 4-disubstituted 1, 2, 3-triazoles bearing organosilicon-sulfur groups via the click reaction sonocatalyzed by LaCuxMn1-xO₃ nanoparticles. *Synth. Commun.* 46, 1595–1604.
- Usmani, Z., Sharma, M., Gupta, P., Karpichev, Y., Gathergood, N., 2020. Ionic liquid based pretreatment of lignocellulosic biomass for enhanced bioconversion. *Bioresour. Technol.* 304. <https://doi.org/10.1016/j.biortech.2020.123003>

- Vasquez, R.P., 1998. Cu₂O by XPS. *Surf. Sci. Spectra* 5, 257–261. <https://doi.org/10.1116/1.1247881>.
- Velpuri, V.R., Muralidharan, K., 2019. Multicomponent click reaction catalyzed by organic surfactant-free copper sulfide (sf-CuS) nano/micro flowers. *J. Organomet. Chem.* 884, 59–65.
- Vibhute, S., Mhaldar, P., Korade, S., Gaikwad, D., Shejawal, R., Pore, D., 2018. Synthesis of magnetically separable catalyst Cu-ACP-Am-Fe₃O₄@SiO₂ for Huisgen 1,3-dipolar cycloaddition. *Tetrahedron Lett.* 59, 3643–3652.
- Wang, C., Ikhlef, D., Kahlal, S., Saillard, J.-Y., Astruc, D., 2016. Metal-catalyzed azide-alkyne “click” reactions: Mechanistic overview and recent trends. *Coord. Chem. Rev.* 316, 1–20.
- Wang, J., Wei, J., Li, J., 2015. Rice straw modified by click reaction for selective extraction of noble metal ions. *Bioresour. Technol.* 177, 182–187. <https://doi.org/10.1016/j.biortech.2014.11.092>.
- Wang, Z., Qin, C., Liu, L., Wang, L., Ding, J., Zhao, W., 2014. Synthesis of Cu_xO (x = 1, 2)/ Amorphous Compounds by Dealloying and Spontaneous Oxidation Method. *Mater. Res.* 17, 33–37.
- Zandipak, R., Ardakani, S.S., Shirzadi, A., 2020. Synthesis and application of nanocomposite Fe₃O₄@SiO₂@CTAB-SiO₂ as a novel adsorbent for removal of cyclophosphamide from water samples. *Sep. Sci. Technol.* 55, 456–470.
- Zarchi, M.A.K., Nazem, F., 2014. One-pot three-component synthesis of 1, 4-disubstituted 1H-1, 2, 3-triazoles using green and recyclable cross-linked poly (4-vinylpyridine)-supported copper sulfate/sodium ascorbate in water/t-BuOH system. *J. Iran. Chem. Soc.* 11, 1731–1742.
- Zhao, R., Liao, Y., Yan, T., Cai, M., 2020. Practical one-pot synthesis of 5-alkynyl-1,2,3-triazoles via heterogeneous copper(I)-catalyzed tandem three-component click/alkynylation reaction. *Appl. Organomet. Chem.* 34, 5319.
- Zirak, M., Gareghshlagi, E.J., 2018. Picolinimidoamide-Cu(II) complex anchored on Fe₃O₄@SiO₂ core-shell magnetic nanoparticles: an efficient reusable catalyst for click reaction. *J. Coord. Chem.* 71, 1168–1179.